PNAS RESEARCH ARTICLE | MICROBIOLOGY ENVIRONMENTAL SCIENCES

Widespread detoxifying NO reductases impart a distinct isotopic fingerprint on N_2O under anoxia

Renée Z. Wang[a,1], Zachery R. Lonergan[b,1], Steven A. Wilbert[b,2], John M. Eiler[a,3], and Dianne K. Newman[a,b,3]

Affiliations are included on p. 7.

Edited by Kyle M. Lancaster, Cornell University, Ithaca, NY; received November 13, 2023; accepted May 10, 2024 by Editorial Board Member Marcetta Y. Darensbourg

Nitrous oxide (N_2O), a potent greenhouse gas, can be generated by multiple biological and abiotic processes in diverse contexts. Accurately tracking the dominant sources of N_2O has the potential to improve our understanding of N_2O fluxes from soils as well as inform the diagnosis of human infections. Isotopic "Site Preference" (SP) values have been used toward this end, as bacterial and fungal nitric oxide reductases (NORs) produce N_2O with different isotopic fingerprints, spanning a large range. Here, we show that flavohemoglobin (Fhp), a hitherto biogeochemically neglected yet widely distributed detoxifying bacterial NO reductase, imparts a distinct SP value onto N_2O under anoxic conditions (~+10‰) that correlates with typical environmental N_2O SP measurements. Using *Pseudomonas aeruginosa* as a model organism, we generated strains that only contained Fhp or the dissimilatory NOR, finding that in vivo N_2O SP values imparted by these enzymes differ by over 10‰. Depending on the cellular physiological state, the ratio of Fhp:NOR varies significantly in wild-type cells and controls the net N_2O SP biosignature: When cells grow anaerobically under denitrifying conditions, NOR dominates; when cells experience rapid, increased nitric oxide concentrations under anoxic conditions but are not growing, Fhp dominates. Other bacteria that only make Fhp generate similar N_2O SP biosignatures to those measured from our *P. aeruginosa* Fhp-only strain. Fhp homologs in sequenced bacterial genomes currently exceed NOR homologs by nearly a factor of four. Accordingly, we suggest a different framework to guide the attribution of N_2O biological sources in nature and disease.

nitrous oxide | nitric oxide | site preference | flavohemoglobin | isotopes

Significance

Nitrous oxide (N_2O) has been found in chronic infection settings and in the atmosphere, where it is a potent greenhouse gas. Microbes are a major source of N_2O; however, determining microbial N_2O sources in diverse habitats is challenging because N_2O is produced by multiple, overlapping pathways. Applying intramolecular isotopic tracing techniques, we identified a unique N_2O isotopic fingerprint that is produced when bacteria encounter nitric oxide (NO) under anoxia in a nongrowing state. Such physiological conditions may be relevant to NO bursts experienced by bacteria infecting human tissues or following wetting events in dryland soils. Our finding motivates future studies to determine the extent to which detoxifying NO reductases may contribute to N_2O biosignatures in diverse environments.

Nitrous oxide (N_2O) is a ubiquitous metabolite present in myriad environments ranging from soils, marine and freshwater systems, and the atmosphere to the human body. Because N_2O can be produced and consumed by multiple microbial nitrogen-cycling processes (1), tracking its sources and fates is challenging. One motivation to do so springs from the fact that N_2O is a potent greenhouse gas, whose current atmospheric concentration is more than 20% compared to preindustrial levels (2); a better understanding of N_2O sources could help facilitate mitigation efforts. Analogously, because N_2O has been measured in chronic pulmonary infections (3), clarity on which pathogens are metabolically active in disease contexts could inform treatment strategies (4).

An intramolecular isotopic fingerprint called "Site Preference" (SP), which measures the relative enrichment of natural abundance ^{15}N in the central (α) vs. terminal (β) nitrogen position in N_2O [Fig. 1*A*; (5)] may be applied for such purposes. Unlike traditional natural abundance isotopic measurements of the total ^{15}N in the bulk molecule (6), SP does not rely on the isotopic composition of the source substrate but instead reflects the reaction mechanism at natural isotopic abundances (7), making it a potentially powerful tool to disentangle N_2O sources in different contexts.

The median values of in situ SP measurements where microbes are present are 10.9 per mille (‰) for soils, 20.9‰ for marine systems, and 23.0‰ for freshwater habitats (Fig. 1*A*). These values are bounded by the median values of in vitro, pure culture studies of N_2O-producing biogenic end-members like bacterial and fungal denitrifiers as well as ammonia-oxidizing bacteria and archaea (AOB and AOA; Fig. 1*A*). Bacterial and fungal denitrifiers are thought to represent two extremes of SP values for N_2O producers with median SP values of –4.3 and 32.2‰ respectively (Fig. 1*A*); this is assumed to reflect the activity of dissimilatory nitric oxide reductases (NOR). In AOB, the SP varies between roughly –11 and 36‰ due to multiple pathways of dissimilatory N_2O formation (8), though recent work showing abiotic N_2O production through spontaneous hybrid formation (10) may complicate this interpretation. In AOA, SP values are roughly 30‰, though

Author contributions: R.Z.W., Z.R.L., J.M.E., and D.K.N. designed research; R.Z.W., Z.R.L., and D.K.N. performed research; S.A.W. contributed new reagents/analytic tools; R.Z.W., Z.R.L., J.M.E., and D.K.N. analyzed data; and R.Z.W., Z.R.L., J.M.E., and D.K.N. wrote the paper.

The authors declare no competing interest.

This article is a PNAS Direct Submission. K.M.L. is a guest editor invited by the Editorial Board.

[1]R.Z.W. and Z.R.L. contributed equally to this work.

[2]Present address: Department of Environmental Health and Engineering, Johns Hopkins, Baltimore, MD 21218.

[3]To whom correspondence may be addressed. Email: eiler@caltech.edu or dkn@caltech.edu.

This article contains supporting information online at https://www.pnas.org/lookup/suppl/doi:10.1073/pnas.2319960121/-/DCSupplemental.

Published June 12, 2024.

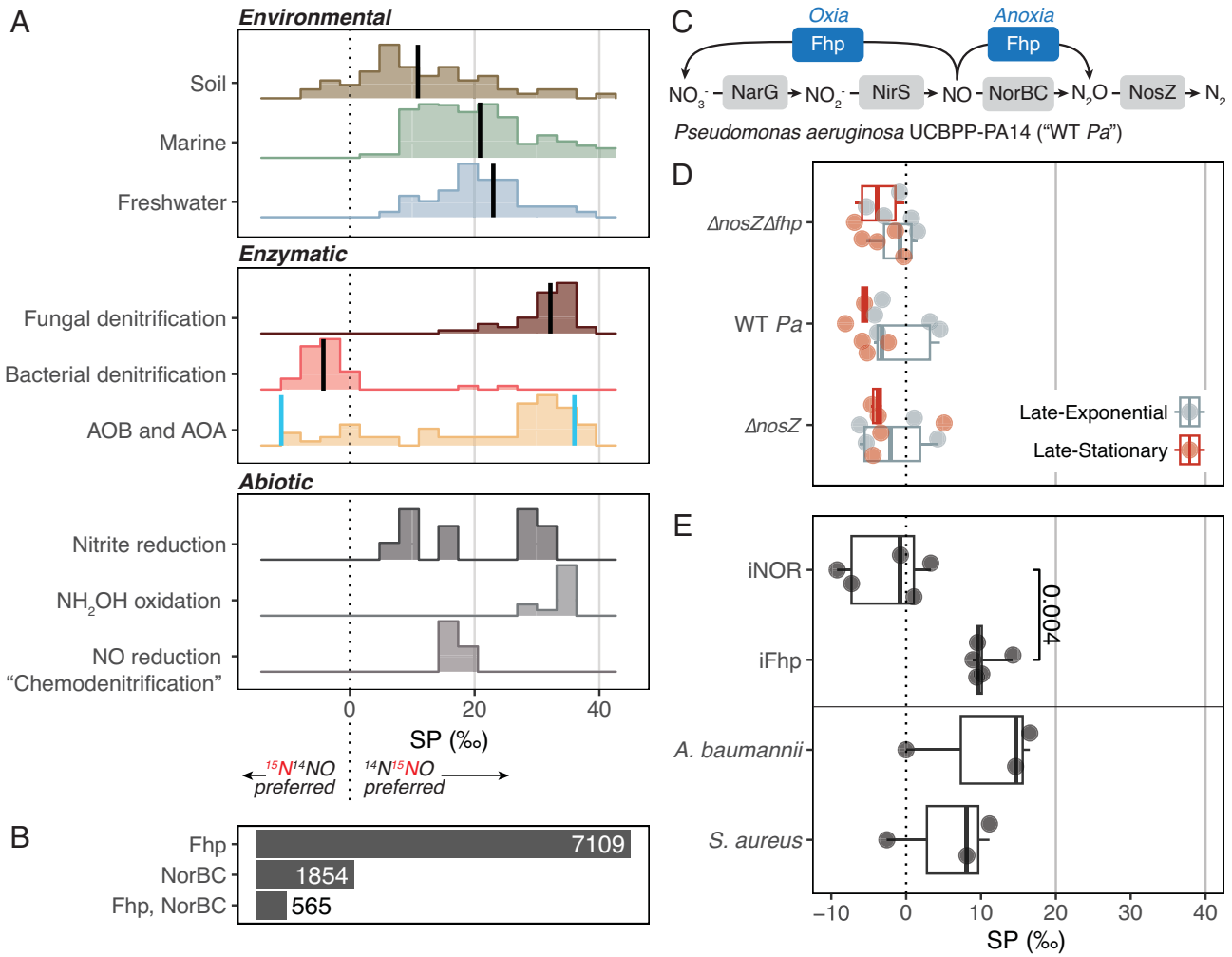

Fig. 1. N_2O production via NO detoxification under anoxic conditions may explain environmental SP values. (*A*) Measured in situ SP values for environmental sources (Soil, Marine, Freshwater) vs. in vitro measurements of N_2O-producing biogenic end-members (bacterial and fungal denitrification, AOB, AOA) and N_2O-producing abiotic reactions; black line shows median; blue lines show end-member values for AOB (8). Histogram height is normalized to each category; see *SI Appendix*, Fig. S11 for outlier values and more details. (*B*) Number of bacterial genomes hits at the phylum level for flavohemoglobin protein (Fhp) and nitrous oxide reductase (NorBC) alone or in combination from Annotree (9); minimum amino acid sequence similarity of 30% was used. See *SI Appendix*, Fig. S1 and Tables S2 and S3 for phylogenetic distribution. (*C*) Relevant N-oxide pathways of *P. aeruginosa* UCBPP-PA14 (*Pa*), the model organism used in this study. *Pa* possesses the full denitrification pathway as well as Fhp. (*D*) SP of N_2O produced by *Pa* and mutant strains with *fhp* and/or *nosZ* genes deleted (Δ*nosZ*Δ*fhp*; Δ*nosZ*) in denitrifying conditions sampled at late-exponential or late-stationary growth phases; see *SI Appendix*, Fig. S2 for more details. (*E*) N_2O SP of *Pa* strains with rhamnose-induced expression of *norBCD* (iNOR) or *fhp* (iFhp) alone as well as *A. baumannii* and *S. aureus*, which only have Fhp. *P* value was calculated via Welch's *t* test. Each data point in (*D* and *E*) represents an individual biological replicate.

current measurements are from enrichment rather than pure cultures (11, 12). In addition, abiotic pathways of N_2O formation display a range of positive SP values, with some displaying intermediate values [~16‰; (13)]. In situ environmental N_2O SP measurements thus likely reflect a mixture of sources, both biotic and abiotic. Toward the goal of deconvolving these potential contributors, our goal in this study was to determine whether another biological N_2O source—one that is linked to nitric oxide (NO) detoxification—may have been overlooked.

Current practices for interpreting SP measurements in natural environments assume that enzymatic N_2O production or consumption is tied to microbial growth. However, an entire other class of enzymes exists that produce N_2O as a consequence of NO detoxification and not for energy conservation (14). Flavohemoglobin proteins (e.g., Fhp/Hmp/Yhb–henceforth referred to as "Fhp") are phylogenetically widespread and protect against NO-mediated toxicity in bacteria and yeast (15). Members of this family are roughly four times more abundant than NORs in annotated bacterial genomes [Fig. 1*B* and *SI Appendix*, Fig. S1 and Tables S1–S3; 7,109 vs. 1,854 genome hits at the phylum level for Fhp vs. NOR using 30% minimum amino acid sequence similarity (9)]. While the ability of Fhp to oxidize NO to nitrate (NO_3^-) under oxic conditions is well known, their capacity to reduce NO to N_2O under anoxic conditions has received less attention (15, 16). Given that bacterial denitrifiers commonly possess both Fhp and NOR (Fig. 1*B* and *SI Appendix*, Table S1), we hypothesized that Fhp might play a role in N_2O emissions and set out to determine whether it imparts a SP onto N_2O distinct from that of bacterial or fungal NORs and AOA or AOB.

Results

Overall SP Values Reflect NOR during Denitrification. To compare the SP of Fhp to NOR in a whole-cell context (in vivo), we used the model bacterial denitrifier, *Pseudomonas aeruginosa* UCBPP-PA14 (*Pa*, Fig. 1*C*). Because this organism is genetically tractable, it provides a means to study the cellular processes of interest in a controlled manner (Table 1). To determine SP values under denitrifying conditions, *Pa*, Δ*nosZ*, and Δ*nosZ*Δ*fhp*—strains with deletions of the nitrous oxide reductase (NOS) gene,

Table 1. Strains studied

Name	Strain description	Fhp?	Nor?	Source
WT *Pa*	Wild-type *P. aeruginosa UCBPP-PA14*	Yes	Yes	Lab Collection
ΔnosZ	Deletion of nitrous oxide reductase gene (*nosZ*, *PA14_20200*) from WT *Pa*	Yes	Yes	This study
ΔnosZΔfhp	Deletion of *nosZ* and flavohemoglobin protein (*fhp*, *PA14_29640*) from WT *Pa*	No	Yes	This study
ΔnorBCΔnosZ	Deletion of nitric oxide reductase (*norBC, PA14_16810,PA14_16830*) and *nosZ* from WT *Pa*	Yes	No	This study
iFhp	Rhamnose-induced expression of *fhp* integrated into the chromosome of WT *Pa* with deletion of native *norBC*, *fhp*, and *nosZ*.	Yes	No	This study
iNOR	Rhamnose-induced expression of the nitric oxide reductase operon, *norBCD* (*PA14_16810*, *PA14_16830*, *PA14_06840*), integrated into the *att* neutral chromosomal site of *Pa* with deletion of native nitrate reductase (*narGHJI*; *PA14_13780-13830*), nitrite reductase (*nirS*; *PA14_06750*), *norBC*, *nosZ*, and *fhp*.	No	Yes	This study
S. aureus	Wild-type *S. aureus* USA300 LAC	Yes	No	Gift
A. baumannii	Wild-type *A. baumannii* ATCC 17978	Yes	No	Gift

The SP of N_2O produced by five strains of *P. aeruginosa* (WT Pa, Δ*nosZ*, Δ*nosZΔfhp*, iFhp, and iNOR) and two wild-type strains of *S. aureus* and *A. baumannii* were measured. See *Materials and Methods* for further details. *S. aureus* and *A. baumannii* were both kindly provided by Eric Skaar, Vanderbilt University Medical Center.

nosZ (*PA14_20200*), and/or *fhp* (*PA14_29640*)—were grown anaerobically in defined medium batch cultures and sampled at late exponential and late stationary growth phases (Table 2, *SI Appendix*, Fig. S2, and *Materials and Methods*). N_2O was cryogenically distilled and analyzed for nitrogen and oxygen isotopes on the Thermo Scientific Ultra High-Resolution Isotope Ratio Mass Spectrometer [HR-IRMS; (17)]; *Materials and Methods*). All isotope data are reported in the delta (δ) notation in units of per mille (‰) where $\delta^{15}N = [(^{15}N/^{14}N)_{sample}/(^{15}N/^{14}N)_{reference} - 1]*1000$ and $SP = \delta^{15}N^{\alpha} - \delta^{15}N^{\beta}$. Values are reported relative to the international reference of AIR for nitrogen; see *Materials and Methods* for more details.

The SP of *ΔnosZΔfhp* should only reflect NOR, since all other known pathways for enzymatic N_2O production and consumption were deleted. The in vivo SP of this strain did not vary significantly by growth phase (Welch's *t* test, $P = 0.2$), and its average value across all growth phases (–2.53 ± 2.90, mean ± SD throughout, $n = 10$) was consistent with prior in vitro measurements of NOR purified from *Paracoccus denitrificans* ATCC 35512 [–5.9 ± 2.1‰, (18)]. The SP of the Δ*norBC*Δ*nosZ* strain, which only has *fhp*, was not measured because it did not grow appreciably in denitrifying conditions (*SI Appendix*, Fig. S2) which is consistent with previous results (19, 20).

Wild-type (WT) *Pa*, which can produce N_2O through both Fhp and NOR (Fig. 1*C*), displayed SP values that did not vary significantly from those observed for the *ΔnosZΔfhp* strain across all growth phases when denitrifying ($P = 0.7$). In addition, the SP of WT *Pa* did not vary significantly by growth phase ($P = 0.07$).

Table 2. Culturing conditions and SP results

Strain	Assay type	Aerobic pregrowth	Anaerobic incubation	SP (‰)	Sample Size (*n*)
iNOR	Suspension	100 mM nitrate	100 mM nitrate, 500 μM DETA NONOate, 305 μM rhamnose	−2.60 ± 5.41	5
iFhp	Suspension	100 mM nitrate	100 mM nitrate, 500 μM DETA NONOate, 305 μM rhamnose	10.45 ± 2.17	5
A. baumannii	Suspension	100 mM nitrate	100 mM nitrate, 500 μM DETA NONOate	10.38 ± 9.05	3
S. aureus	Suspension	100 mM nitrate	100 mM nitrate, 500 μM DETA NONOate	5.56 ± 7.21	3
ΔnosZ	Batch; End-exponential	100 mM nitrate	100 mM nitrate	−1.56 ± 5.04	4
	Batch; End-stationary	100 mM nitrate	100 mM nitrate	−2.21 ± 4.10	5
ΔnosZΔfhp	Batch; End-exponential	100 mM nitrate	100 mM nitrate	−1.39 ± 2.78	5
	Batch; End-stationary	100 mM nitrate	100 mM nitrate	−3.68 ± 2.81	5
WT *Pa*	Batch; End-exponential	100 mM nitrate	100 mM nitrate	−0.70 ± 4.19	5
	Batch; End-stationary	100 mM nitrate	100 mM nitrate	−5.43 ± 2.04	5
	Suspension	100 μM DETA NONOate	500 μM DETA NONOate	−2.59 ± 7.53	2
	Suspension	100 μM DETA NONOate + 100 mM nitrate	500 μM DETA NONOate	9.14 ± 3.70	2
	Suspension	100 mM nitrate	500 μM DETA NONOate + 100 mM nitrate	2.61 ± 9.31	5
	Batch; End-stationary	100 mM nitrate	500 μM DETA NONOate + 100 mM nitrate	−3.34 ± 0.83	2

All strains were grown in aerobic pregrowths before being resuspended in fresh media and anoxically incubated for headspace sampling as batch culture or suspension assays (*SI Appendix*, Fig. S12); nitrate and/or DETA NONOate ($C_4H_{13}N_5O_2$) was supplemented to provide endogenous vs. exogenous NO, respectively. See *Materials and Methods* for more details. SP values (mean ± SD) of *n* biological replicates; see Dataset S1 for full results.

The SP of Δ*nosZ* was also measured because prior studies showed that NOS can increase the SP of the residual N_2O pool through preferential cleavage of the ^{14}N-O vs. ^{15}N-O bond in N_2O (21, 22); however, SP values of Δ*nosZ* were similar to Δ*nosZ*Δ*fhp* ($P = 0.7$) and did not vary by growth phase ($P = 0.8$; Fig. 1*D*). Therefore, even though Fhp was likely present in all previously measured bacterial denitrifier strains for in vitro measurements (*SI Appendix*, Table S2), it does not affect the overall SP value when strains are grown under denitrifying conditions, suggesting that NOR dominates the isotopic signature under these conditions (*Discussion*). However, the potential for Fhp to impact the SP of N_2O under other conditions remained open.

Fhp Has an Intermediate, Positive SP Value Compared to Bacterial and Fungal NORs. To distinguish the SP of Fhp and NOR, we engineered two *Pa* strains possessing only Fhp or NOR that could be induced in the presence of rhamnose; inducible Fhp ("iFhp") and NOR ("iNOR") functionality was validated by complementation experiments (Table 1 and *SI Appendix*, Fig. S3). Since these strains lack denitrification enzymes and are incapable of anaerobic growth, suspension assays were developed to culture bacteria aerobically while inducing gene expression prior to placement in nongrowing, anoxic conditions. Strains were provided exogenous NO via the small molecule donor DETA NONOate ($C_4H_{13}N_5O_2$) at subtoxic concentrations (*SI Appendix*, Fig. S4) and then incubated under anoxic conditions for 24 h at 37 °C before the headspace was sampled; see Table 2 and *Materials and Methods* for more details.

Under these conditions, iFhp displayed SP values (10.45 ± 2.17‰, $n = 5$) that were significantly more positive than iNOR (−2.60 ± 5.41‰, $n = 5$; $P = 0.004$; Fig. 1 *E*, *Top*). iNOR values were also consistent with both our Δ*nosZ*Δ*fhp* denitrifying growth SP measurements and prior in vitro NOR SP measurements (18). In addition, we observe a large variation (on the order of 10‰) in SP between biological replicates of NOR, in agreement with prior studies (−5 and −9‰; $n = 2$ in ref. 18). This variation neither correlates with the degree of nitrate consumption for Δ*nosZ*Δ*fhp*, nor N_2O production for Δ*nosZ*Δ*fhp* and iNOR (*SI Appendix*, Fig. S5), indicating that this variation in SP may be inherent to NOR.

Next, to validate Fhp SP values outside *Pa*, two wild-type, non-denitrifying strains with only Fhp, *Staphylococcus aureus* USA300 LAC, and *Acinetobacter baumannii* ATCC 17978 were also measured. Fhp from *S. aureus* (named Hmp in this organism) has 31.6% amino acid sequence similarity to Fhp from *P. aeruginosa*, while Fhp from *A. baumannii* has 98.5% similarity. However, all Fhps share a common catalytic site for NO binding and reduction, a globin module with heme B (15), that is responsible for imparting the observed SP. The SP of *S. aureus* (5.56 ± 7.21‰, $n = 3$) and *A. baumannii* (10.38 ± 9.05‰, $n = 3$) were both positive and statistically indistinguishable from *Pa* iFhp (Fig. 1 *E*, *Bottom*). In addition, the variation in SP values for Fhp (on the order of 10‰) is similar to that of NOR, implying that there is an inherent variation in SP for these enzymes, though addressing this variation is outside the scope of this current study.

Exogenous NO Shifts SP Values toward Fhp. Given the potential for Fhp to impart a positive SP distinct from NOR, we next sought to identify physiological conditions where it might dominate the N_2O isotopic fingerprint in the wild-type. Historically, N_2O isotopic measurements from pure cultures have been made for actively growing cells, which would amplify isotopic signatures imparted by catabolic enzymes like NOR. Yet, evidence is mounting that slow, survival physiology dominates microbial existence in diverse habitats (23, 24), motivating N_2O SP measurement during nongrowth conditions.

To test whether *Pa* can produce positive SP values indicative of Fhp activity, we grew WT *Pa* in denitrifying batch cultures and nongrowing, anoxic suspensions with varying combinations of nitrate (NO_3^-) and DETA NONOate to provide NO endogenously via denitrification and/or exogenously via small molecule-mediated NO release (Fig. 2*A*), which we hypothesized would promote NOR or Fhp activity. We validated the induction of NOR and Fhp using quantitative unlabeled proteomics (*Materials and Methods*) and calculated the ratios of Fhp to NOR to quantify relative changes of each NO reductase. In denitrifying, batch culture conditions (Fig. 2*B*), the ratio of Fhp to NOR was less than one (~0.25) and did not significantly change upon addition of NO ($P = 0.09$; Fig. 2*B*). By contrast, NorB, which contains the catalytic subunit of NOR, was undetectable before NO addition in the suspension assays (*SI Appendix*, Fig. S6), which were performed by shifting oxic pregrown cultures to nongrowing, anoxic conditions. Although NorB increased to detectable levels upon the addition of DETA NONOate (*SI Appendix*, Fig. S6), Fhp was far more abundant, leading to a high ratio of Fhp to NOR (~3, Fig. 2*C*).

Paired SP and $\delta^{15}N^{bulk}$ data allowed us to track which pool of NO was used by Fhp or NOR for N_2O production (*SI Appendix*, Fig. S7 and Fig. 2 *C* and *D*). When N-oxides are reduced to N_2O, $\delta^{15}N^{bulk}$ retains the isotopic signature of the original N (25). Specifically, nitrate had a $\delta^{15}N$ value of 0.40 ± 1.28 and DETA NONOate had a $\delta^{15}N$ value of −22.95 ± 0.15‰; non-WT *Pa* strains grown as batch cultures with only nitrate or incubated as suspension assays with DETA NONOate retained these distinct signatures in their $\delta^{15}N^{bulk}$ values (−27.4 ± 1.4 vs. −91.0 ± 6.5‰, respectively, *SI Appendix*, Fig. S8). When WT *Pa* was incubated anoxically with either nitrate or DETA NONOate, $\delta^{15}N^{bulk}$ values correspondingly showed only one NO source (Fig. 2*C*); when given both substrates simultaneously, N_2O could be made from varying ratios of both exogenous and endogenous NO.

SP data (Fig. 2*D*) were consistent with denitrifying cultures favoring NOR production, and nongrowing, anoxic suspensions favoring Fhp. When WT *Pa* was grown under denitrifying conditions, SP values were more negative and within the range of iNOR. However, in suspension assays, SP values spanned the range from iNOR to iFhp, consistent with increased Fhp abundance in these conditions. The most positive SP values, within the range of iFhp, were seen when WT *Pa* was given a high dose of both endogenous and exogenous NO in oxic pregrowth (nitrate and DETA NONOate, blue stars, *SI Appendix*, Fig. S7) followed by anoxic incubation with exogenous NO (DETA NONOate only, blue circles, Fig. 2*D*).

Discussion

Toward the goal of attributing N_2O sources more accurately in complex environments, from soils to human infections, it is imperative to be aware of all possible biotic and abiotic processes that may contribute to N_2O production. Until this work, studies of N_2O generation by biological sources have focused on catabolic enzymes, yet non-growth-related enzymes may be equally important under some conditions. Our results suggest that in environments where organisms are not growing yet experience a burst of NO production following oxic growth, Fhp homologs have the potential to contribute to N_2O emissions. While further research will be needed to determine whether this is in fact the case in nature or disease, these findings motivate consideration of a hitherto neglected N_2O source.

Given that Fhp homologs are present in many denitrifying bacteria and AOB (*SI Appendix*, Figs. S1 and S9 and Tables S1–S3), our results indicate that Fhp has the potential to have contributed to enzymatic N_2O production and SP values measured in previous

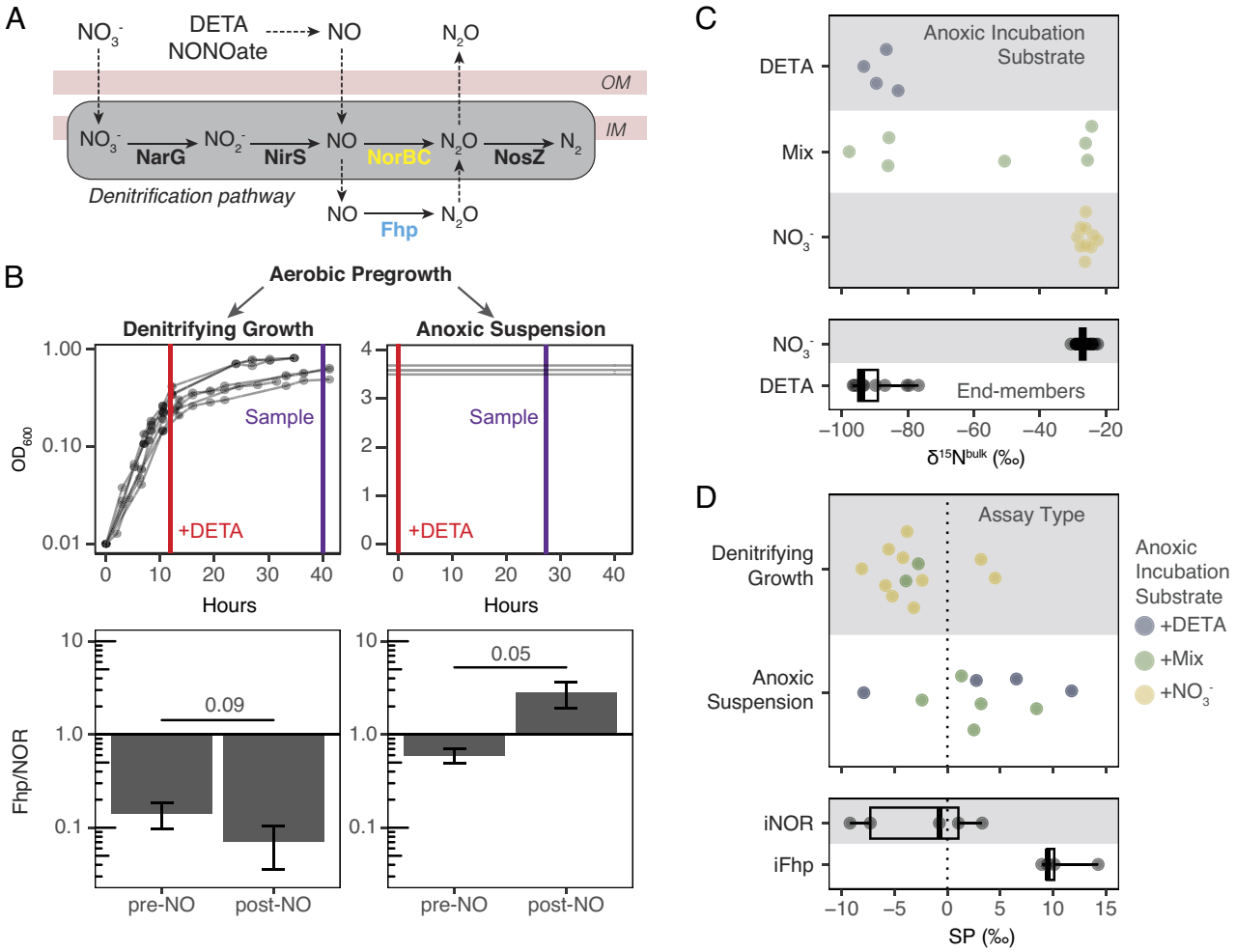

Fig. 2. High concentrations of NO shift SP values toward Fhp. (*A*) In *Pa*, NorBC contributes to overall cell energetics as part of the denitrification pathway; Fhp does not and is primarily used for NO detoxification; OM and IM denote the bacterial outer vs. inner membrane. (*B*) After aerobic pregrowth, WT *Pa* was cultured anaerobically via two assay types i) to maximize growth via denitrification ("Denitrifying Growth," *Left*) or ii) as nongrowing cells in suspension assays ("Anoxic Suspension," *Right*; see *SI Appendix*, Fig. S12 for more details). Exogenous NO was supplied through DETA NONOate (red lines) and headspace was then sampled for SP analysis (purple lines). Culture aliquots for proteomics analysis were taken immediately prior to NO addition ("pre-") or during the same time as headspace sampling ("post-NO"). Ratio of Fhp to NOR in these conditions is shown as bar charts below; see *SI Appendix*, Fig. S6 for full results. *P* values were calculated via Welch's *t* test. (*C*) $\delta^{15}N^{bulk}$ values for WT *Pa* incubated anoxically with DETA NONOate (blue), nitrate (yellow) or both (green); end-member values are from non-WT *Pa* strains incubated with only nitrate or DETA as an NO source (*SI Appendix*, Fig. S8). (*D*) SP measurements for WT *Pa* grown as denitrifying growths or anoxic suspensions, as illustrated in (*B*). Colors indicate anoxic incubation substrate and are the same as panel (*C*). iNOR and iFhp SP values are from Fig. 1*E*. For (*C* and *D*), box plots indicate median, upper, and lower quartiles, and extreme values.

studies if cells were in nongrowing states. Notably, all prior reports of SP from bacterial denitrifiers (putatively NOR-only) used strains that also have Fhp (*SI Appendix*, Table S1); given the sensitivity of enzyme abundance to the physiological state during the time of measurement, it is plausible that the positive spread in SP values observed in these studies (26) may reflect cryptic Fhp activity. An Fhp homolog, Yhb, exists in yeast (15) and is present in previously studied fungal denitrifiers as well (*SI Appendix*, Table S4), possibly contributing to the tail toward 10‰ observed from the literature (Fig. 1*A*), assuming the SP signature of Yhb is similar to that of Fhp. In addition, our isotopic results show that when cells are grown in denitrifying conditions, NOR dominates the SP signal (Fig. 2*D*). This may explain why prior studies of denitrifiers with Fhp gave SP values consistent with NOR—as a result of growing strains in conditions that favor NOR, SP will inevitably reflect NOR and not Fhp. This is consistent with the relative kinetic rates of Fhp and NOR: In oxic conditions, Fhp is highly efficient at converting NO in nitrate [V_{max} = 670 s^{-1}; K_M = 0.28 μM (27)] but in anoxic conditions, Fhp's turnover rate is reduced to about 1% of its oxic rate [0.2 to 0.1 s^{-1}; (27–29)]. Therefore, as shown in prior studies of *Pseudomonas*, in anoxic, denitrifying conditions NOR outcompetes Fhp for NO (30).

The strength of NOR's SP signal during denitrification begs the question—under what conditions would Fhp meaningfully contribute to the overall SP value measured in a complex habitat? In our study, we find that Fhp-like SP values in WT *Pa* are observed when cells are in a nongrowth condition before being exposed to exogenous NO (Fig. 2*D* and *SI Appendix*, Fig. S7). Because NOR is primarily used for growth through denitrification, a nongrowth state limits the influence of NOR and allows Fhp activity to dominate the total N_2O SP. There is substantial evidence that most microbes exist in nongrowing states in natural environments (23, 24), presenting opportunities for Fhp to contribute to environmental N_2O SP values, along with organisms engaged in nitrification and denitrification. For example, soils can experience climate extremes that promote distinct metabolisms, where soil drying selects for slow growth and survival, and wetter soils promote increased growth rates (31, 32). Interestingly, N_2O is detectable even in drought-affected, oxygenated soils and increases after wetting (33). Similarly, "pulses" (short, high-concentration bursts) of NO on the order of 0.1 to 1 nmol

N m^{-2} s^{-1} have been detected after wetting of dryland soils (34, 35) and in incubated soils even when denitrification is occurring (36). In addition, opportunistic pathogens are thought to experience NO bursts from different cell types in the human immune system (37). Consistent with these environmental concentrations, Fhp expression is detectable at nanomolar NO concentrations (38). Yet, to speculate on whether such pulses may trigger Fhp activity requires an ability to track dynamic NO and oxygen concentrations in situ. Ultimately, knowledge of the relative abundance of N_2O-generating enzymes, paired with knowledge of microscale environmental states and the relative rates of N_2O generation by abiotic and biotic processes, will be necessary to attribute sources with confidence.

Finally, we note that Fhp is phylogenetically widespread, more abundant than NOR, and present in organisms classified as obligate aerobes; therefore, measuring Fhp values from a representative group of diverse bacteria may illuminate the natural variation in SP values. In addition, measuring other NO-detoxifying proteins may shed further light on the SP values of this neglected class of noncatabolic enzymes. Flavo-diiron proteins, which only operate in anoxic conditions and only reduce NO to N_2O for detoxification (14) present an attractive next target for SP measurements. Further detailed studies of Fhp's reaction mechanism paired with SP data are needed to understand what determines the SP of N_2O formation through NO reduction (7, 13, 39, 40). Though this manuscript focuses on N_2O, the general approach presented here exemplifies how particular microbial metabolic pathways may be forensically distinguished by means of intramolecular isotopic biosignatures within their products. Going forward, we envision that such an approach, when applied to other metabolites of interest, may help us better understand how microbial activities, in comparison to abiotic processes, shape diverse habitats, from soils to animal hosts.

Materials and Methods

Medium and Nitric Oxide Donors. Synthetic cystic fibrosis medium ("Base SCFM") (41) was amended with 20 mM sodium succinate and trace metals to increase cell and N_2O yields ("SCFM Amended" or "SCFM-A"; see *SI Appendix*). All strains in this study were grown in SCFM-A media. The small-molecule NO donor DETA NONOate ($C_4H_{13}N_5O_2$, #82120 Cayman Chemical Company) was used in certain experiments.

Strain Generation. We measured the SP of N_2O produced by five strains of *Pa* and two wild-type strains of *S. aureus* and *A. baumannii* (Table 1). *P. aeruginosa* UCBPP-PA14 was the wild-type (WT) and parent strain of all genetic manipulations done in this study. Individual and combinatory mutants of *Pa* nitrate reductase (*ΔnarGHJI*; *PA14_13780-13830*), nitrite reductase (*ΔnirS*; *PA14_06750*), nitric oxide reductase (*ΔnorBC*; *PA14_16810*, *PA14_16830*), and nitrous oxide reductase (*ΔnosZ*, *PA14_20200*) were generated previously (19). *ΔnosZΔfhp* has the additional deletion of *fhp*, the flavohemoglobin protein/nitric oxide dioxygenase (*PA14_29640*). Clean deletions were done using allelic exchange as previously described (42). Strains with inducible *fhp* ["iFhp," to denote *P. aeruginosa ΔnosZΔfhpΔnor att::mTn7*(GentR,*fhp*)] and *norBCD* ["iNOR," to denote *P. aeruginosa ΔnarΔnirΔnorΔnosZΔfhp att::mTn7*(GentR,*norBCD*)] (Table 1) were generated by, first, amplifying *fhp* or *norCBD* from *P. aeruginosa* genomic DNA. See *SI Appendix*, Table S5 for primers used. PCR products were ligated into plasmid the miniTn7 plasmid pJM220 (43) via Gibson cloning (44) 3′ of the *rhaB* promoter for rhamnose-specific expression. Plasmids were delivered to *P. aeruginosa* via triparental conjugation with *Escherichia coli* SM10(λpir) and SM10(λpir) pTNS1 (43), and exconjugants were selected on LB agar supplemented with chloramphenicol (10 μg/mL) and gentamicin (20 μg/mL) and verified by PCR. In addition, we measured the SP of N_2O produced by two wild-type, nondenitrifying bacteria with only *fhp/hmp* annotated in their genomes–*S. aureus* USA300 LAC (putative flavohemoprotein *SAUSA300_0234*) and *A. baumannii* ATCC 17978 (putative flavohemoprotein *A1S_3085*), both kindly provided by Eric Skaar, Vanderbilt University Medical Center.

Culturing Conditions. iNOR, iFhp, and non-*Pseudomonas* strains were first screened for N_2O production before scaling up the culturing process for isotopic measurement (*SI Appendix*, Table S2). Strains were then grown in one of two ways: i) suspension assays or ii) batch culture (*SI Appendix*, Fig. S12). For suspension assays, strains were first grown in shaking, aerobic pregrowths for 16 h at 37 °C (OD_{600} ~3 to 4) in 150 mL SCFM-A. The aerobic pregrowths for iNOR, iFhp, *A. baumannii*, and *S. aureus* were supplemented with 100 mM KNO_3. In WT *Pa* suspension assays, pregrowth was supplemented with either 100 μM DETA NONOate, 100 μM DETA NONOate, and 100 mM KNO_3 or 100 mM KNO_3. Next, cells were transferred to 50 mL conical tubes, pelleted for 15 min at 23 °C and 6,800 x g, and resuspended in 150 mL of fresh SCFM-A. Then, 500 μM DETA NONOate was added to iNOR, iFhp, *A. baumannii*, and *S. aureus* experiments; iNOR and iFhp were also supplemented with 305 μM L-rhamnose monohydrate [$C_6H_{12}O_5 \cdot H_2O$ (Sigma-Aldrich R3875-25G)] to promote rhamnose-inducible expression of *norBCD* or *fhp*. For WT *Pa* suspension assays, either 500 μM DETA NONOate or 500 μM DETA NONOate and 100 mM KNO_3 were added. Following the suspension setup, vacuum flask headspace was purged with N_2 gas to establish anoxia, and flasks were incubated statically for 24 h at 37 °C before headspace sampling. See *SI Appendix*, Fig. S14 for more details. For batch culture assays, strains were first grown in aerobic pregrowths of 5 mL SCFM-A with 100 mM KNO_3 for 16 h at 37 °C, 250 rpm shaking (OD_{600} ~ 3 to 4). Cells were then diluted to OD_{600} = 0.01 in vacuum flasks with 150 mL of SCFM-A. For *ΔnosZ* and *ΔnosZΔfhp*, 100 mM of KNO_3 was added. For WT *Pa*, either 100 mM KNO_3 or 500 μM DETA NONOate and 100 mM KNO_3 were added. Since *Pa* is the only denitrifying organism tested, a concentration sweep of KNO_3 was performed ranging from 20 to 100 mM; no significant growth changes were observed, so we continued with 100 mM to ensure KNO_3 was never limited (*SI Appendix*, Fig. S19). Then, 100 mM KNO_3 concentrations are also consistent with prior SP studies (i.e., ref. 26), which used high KNO_3 concentrations to ensure adequate amounts of N_2O were produced for isotopic analysis. Vacuum flask headspace was purged with N_2 gas to establish anoxia and incubated statically at 37 °C. Flasks were sampled twice: first, approximately 12 h at end-exponential growth and second, approximately 40 h at end-stationary. One WT *Pa* batch culture experiment, where 500 μM DETA NONOate and 100 mM KNO_3 were added to the vacuum flask, was only sampled at ~40 h after the DETA NONOate was added at ~12 h. See *SI Appendix*, Fig. S12 for more details. Additional moles of nitrate were accidentally added in the Aug192021 batch for a final concentration of 233 mM nitrate (*SI Appendix*, Table S7); however, no difference in SP was observed (Fig. 1*D*).

Headspace Sampling and N_2O Distillation. N_2O was distilled from the headspace samples on an ultratorr vacuum line prior to isotopic analysis. Noncondensable gases (i.e., N_2, Ar) were removed by submerging the sample in a liquid nitrogen trap and removing the noncondensed gases; carbon dioxide was removed using an Ascarite II CO_2 Absorbent (Thermo Scientific) trap, and water was removed by condensation on an ethanol and dry ice slurry trap; see *SI Appendix*, Fig. S14 for more details. After headspace distillation, low-volume samples from multiple flasks were combined for subsequent isotopic analysis; see extended dataset for which samples and how many flasks were combined. Two vacuum distillation blanks (DistillationBlank-1, DistillationBlank-2) and a no-cells vacuum flask blank (FlaskBlank-1) were measured to test whether the distillation process causes significant isotopic fractionation (*SI Appendix*, Table S8). DistillationBlank-1 and 2 showed little difference from the original N_2O gas (roughly 0.1 ± 0.5‰ difference, *SI Appendix*, Table S8), indicating that the distillation process does not significantly fractionate our target gas. FlaskBlank-1 showed a −2.25 ± 0.90‰ difference in $\delta^{18}O$; this may have been caused by the exchange of O isotopes between the incubated N_2O gas and H_2O–therefore, our study relies on the interpretation of the N isotopes instead.

SP Measurements. All isotopic measurements in this study are reported in the delta notation (δ) in units of per mille (‰) where $\delta^{15}N = [(^{15}R_{sam}/^{15}R_{ref} - 1)*1000]$, where ^{15}R is the ratio of $^{15}N/^{14}N$ in the sample ("sam") or reference ("ref"). All values here are reported to the international reference of Air for nitrogen. SP is as defined in refs. 5 and 45, where $SP \equiv \delta^{15}N^{\alpha} - \delta^{15}N^{\beta}$, the difference in $\delta^{15}N$ between the central (α) and terminal (β) nitrogen; see *SI Appendix* for more details. Measurements were performed on two Thermo Scientific Ultra HR-IRMS. All measurements were corrected for background noise (17) and $^{13}C^{16}O_2$ at Mass 45; see *SI Appendix* for more details. Shot noise error (17) was calculated for

each measurement and compared to the observed SD to ensure measurements were reaching shot noise limits (*SI Appendix*, Fig. S15). "Zero enrichment" tests where the reference gas is measured as a sample against itself were also regularly performed over the course of the study to ensure pressure balance across a range of sample sizes (*SI Appendix*, Fig. S16). Two samples were also measured across both HR-IRMS instruments to ensure measurement consistency across instruments (*SI Appendix*, Fig. S17). Finally, all samples were corrected for "scrambling" following (5, 45); see *SI Appendix* for more details.

Isotopic Measurement of DETA NONOate and Nitrate. $\delta^{15}N$ of nitrate and the full vs. decayed DETA NONOate molecule were measured on a Delta-V Advantage with Gas Bench and Costech elemental analyzer. The $\delta^{15}N$ of the released NO molecules by DETA NONOate was then calculated through mass balance (*SI Appendix*). For all measurements, the instrument was tuned with an internal standard to ensure instrument sensitivity and linearity and to ensure correct measurement mass position. Three analytical replicates of each sample were measured. All samples were bracketed at the beginning and end of the run by a suite of external isotope standards (Urea $\delta^{15}N = 0.0‰$; Acetanilide $\delta^{15}N = 19.56 \pm 0.03‰$; all reported vs. AIR), tin capsule blanks, and NaOH and HCl blanks. After correcting for blanks, measured $\delta^{15}N$ values were then corrected to reported values vs. AIR using the external Urea and Acetanilide standards.

Phylogram and AnnoTree Search Parameters. A phylogram of species with annotated Fhp/Hmp sequences was first made from the NCBI database (*SI Appendix*, Fig. S1 and Table S13). Phylogram was made to include representative strains from a range of known bacterial species. The amino acid sequence of Fhp from *P. aeruginosa* UCBPP-PA14 was used (*PA14_29640*). Default NCBI protein BLAST blastp parameters were used to identify Fhp orthologs. Protein sequences were collected, and a simple phylogeny was constructed using EMBL-EBI Simple Phylogeny tool with default parameters and neighbor-joining clustering (46). Fhp and NorBC were also queried from AnnoTree, a functionally annotated database of >27,000 bacterial and >1,500 archaeal genomes (9). The default search parameters were used: % identity: 30; E value: 0.00001; % subject alignment: 70; % query alignment: 70. Results are shown in *SI Appendix*, Tables S1–S3 at the phylum level.

Proteomics. Cells were collected in 5 mL aliquots from batch denitrifying or anoxic suspension assays immediately prior to DETA NONOate addition (*SI Appendix*, Fig. S4, red line) or after 24 to 28 h incubation with DETA-NONOate (*SI Appendix*, Fig. S12, purple line) and centrifuged at 6,800 x g, and pellets were frozen at −80 °C. Thawed pellets were processed and digested via S-Trap™ (ProtoFi, LLC, Fairport, NY) micro protocol digestion (*SI Appendix*). LC–MS analysis of digested peptides was performed on an EASY-nLC 1200 (Thermo Fisher Scientific, San Jose, CA) coupled to a Q Exactive HF Orbitrap mass spectrometer (Thermo Fisher Scientific, Bremen, Germany) equipped with a Nanospray Flex ion source: 500 ng peptides of each sample were directly loaded onto an Aurora 25 cm × 75 μm ID, 1.6 μm C18 column (Ion Opticks) heated to 50 °C. The peptides were separated with a 2 h gradient at a flow rate of 350 nL/min as follows: 2 to 6% solvent B (7.5 min), 6 to 25% B (82.5 min), 25 to 40% B (30 min), 40 to 98% B (1 min), and held at 98% B (12 min). Solvent A consisted of 97.8% H_2O, 2% ACN, and 0.2% formic acid, and solvent B consisted of 19.8% H_2O, 80% ACN, and 0.2% formic acid. The Q Exactive HF was operated in data-dependent mode with Tune (version 2.8 SP1 build 2806) instrument control software; see *SI Appendix* for measurement parameters. Data analysis was performed using Thermo Proteome Discoverer 2.5 (Thermo Fisher Scientific, San Jose, CA) with a SEQUEST algorithm (PMID 24226387). The data were searched against the *P. aeruginosa* UCBPP-PA14 proteome (UP000002438) acquired from UniProtKB (PMID: 36408920) in 2022-2-09; see *SI Appendix* for search parameters. Protein abundances were reported using ms1 feature-based label-free quantitation. The median abundance for each sample was normalized to the same value.

Data, Materials, and Software Availability. All study data are included in the article and/or supporting information.

ACKNOWLEDGMENTS. We thank Colette L. Kelly for valuable guidance and help with the scrambling correction; Nami Kitchen for assistance with IRMS measurements; Nathan Hart at the Caltech Glass Shop for building the vacuum flasks; and Joachim Mohn for external nitrous oxide reference gasses. We thank Dr. Tsui-Fen Chou and Baiyi Quan at the Caltech Proteome Exploration Laboratory for assistance with proteomics-based experiments. NSF Graduate Research Fellowship Program (R.Z.W.), Jane Coffin Childs Memorial Fund for Medical Research Fellowship (Z.R.L.), and NIH grant R01 HL152190-03 (J.M.E. and D.K.N.)

Author affiliations: [a]Division of Geological and Planetary Sciences, Caltech, Pasadena, CA 91101; and [b]Division of Biology and Biological Engineering, Caltech, Pasadena, CA 91101

1. M. M. M. Kuypers, H. K. Marchant, B. Kartal, The microbial nitrogen-cycling network. *Nat. Rev. Microbiol.* **16**, 263–276 (2018).
2. H. Tian *et al.*, A comprehensive quantification of global nitrous oxide sources and sinks. *Nature* **586**, 248–256 (2020).
3. M. Kolpen *et al.*, Nitrous oxide production in sputum from cystic fibrosis patients with chronic Pseudomonas aeruginosa lung infection. *PLoS One* **9**, e84353 (2014).
4. G. M. Cook, C. Greening, K. Hards, M. Berney, Energetics of pathogenic bacteria and opportunities for drug development. *Adv. Microb. Physiol.* **65**, 1–62 (2014).
5. S. Toyoda, N. Yoshida, Determination of nitrogen isotopomers of nitrous oxide on a modified isotope ratio mass spectrometer. *Anal. Chem.* **71**, 4711–4718 (1999).
6. T. R. A. Denk *et al.*, The nitrogen cycle: A review of isotope effects and isotope modeling approaches. *Soil Biol. Biochem.* **105**, 121–137 (2017).
7. Z. Wang, E. A. Schauble, J. M. Eiler, Equilibrium thermodynamics of multiply substituted isotopologues of molecular gases. *Geochim. Cosmochim. Acta* **68**, 4779–4797 (2004).
8. C. H. Frame, K. L. Casciotti, Biogeochemical controls and isotopic signatures of nitrous oxide production by a marine ammonia-oxidizing bacterium. *Biogeosciences* **7**, 2695–2709 (2010).
9. K. Mendler *et al.*, AnnoTree: Visualization and exploration of a functionally annotated microbial tree of life. *Nucleic Acids Res.* **47**, 4442–4448 (2019).
10. J. A. Kozlowski, M. Stieglmeier, C. Schleper, M. G. Klotz, L. Y. Stein, Pathways and key intermediates required for obligate aerobic ammonia-dependent chemolithotrophy in bacteria and Thaumarchaeota. *ISME J.* **10**, 1836–1845 (2016).
11. A. E. Santoro, C. Buchwald, M. R. McIlvin, K. L. Casciotti, Isotopic signature of N_2O produced by marine ammonia-oxidizing archaea. *Science* **333**, 1282–1285 (2011).
12. M.-Y. Jung *et al.*, Isotopic signatures of N_2O produced by ammonia-oxidizing archaea from soils. *ISME J.* **8**, 1115–1125 (2014).
13. C. L. Stanton *et al.*, Nitrous oxide from chemodenitrification: A possible missing link in the Proterozoic greenhouse and the evolution of aerobic respiration. *Geobiology* **16**, 597–609 (2018).
14. C. Ferousi, S. H. Majer, I. M. DiMucci, K. M. Lancaster, Biological and Bioinspired Inorganic N-N bond-forming reactions. *Chem. Rev.* **120**, 5252–5307 (2020).
15. R. K. Poole, M. N. Hughes, New functions for the ancient globin family: Bacterial responses to nitric oxide and nitrosative stress. *Mol. Microbiol.* **36**, 775–783 (2000).
16. A. Bonamore, A. Boffi, Flavohemoglobin: Structure and reactivity. *IUBMB Life* **60**, 19–28 (2008).
17. J. M. Eiler *et al.*, A high-resolution gas-source isotope ratio mass spectrometer. *Int. J. Mass Spectrom.* **335**, 45–56 (2013).
18. T. Yamazaki *et al.*, Isotopomeric characterization of nitrous oxide produced by reaction of enzymes extracted from nitrifying and denitrifying bacteria. *Biogeosciences* **11**, 2679–2689 (2014).
19. S. A. Wilbert, D. K. Newman, The contrasting roles of nitric oxide drive microbial community organization as a function of oxygen presence. *Curr. Biol.* **32**, 5221–5234.e4 (2022).
20. S. S. Yoon *et al.*, *Pseudomonas aeruginosa* anaerobic respiration in biofilms: Relationships to cystic fibrosis pathogenesis. *Dev. Cell* **3**, 593–603 (2002).
21. K. L. Casciotti *et al.*, Nitrous oxide cycling in the Eastern Tropical South Pacific as inferred from isotopic and isotopomeric data. *Deep Sea Res. Part II Top. Stud. Oceanogr.* **156**, 155–167 (2018).
22. N. E. Ostrom *et al.*, Isotopologue effects during N_2O reduction in soils and in pure cultures of denitrifiers. *J. Geophys. Res.* **112**, G02005 (2007).
23. A. Bodor *et al.*, Challenges of unculturable bacteria: Environmental perspectives. *Rev. Environ. Sci. Biotechnol.* **19**, 1–22 (2020).
24. M. Bergkessel, D. W. Basta, D. K. Newman, The physiology of growth arrest: Uniting molecular and environmental microbiology. *Nat. Rev. Microbiol.* **14**, 549–562 (2016).
25. D. M. Sigman *et al.*, A bacterial method for the nitrogen isotopic analysis of nitrate in seawater and freshwater. *Anal. Chem.* **73**, 4145–4153 (2001).
26. S. Toyoda, H. Mutobe, H. Yamagishi, N. Yoshida, Y. Tanji, Fractionation of N_2O isotopomers during production by denitrifier. *Soil Biol. Biochem.* **37**, 1535–1545 (2005).
27. A. M. Gardner, L. A. Martin, P. R. Gardner, Y. Dou, J. S. Olson, Steady-state and transient kinetics of *Escherichia coli* nitric-oxide dioxygenase (flavohemoglobin). The B10 tyrosine hydroxyl is essential for dioxygen binding and catalysis. *J. Biol. Chem.* **275**, 12581–12589 (2000).
28. S. O. Kim, Y. Orii, D. Lloyd, M. N. Hughes, R. K. Poole, Anoxic function for the *Escherichia coli* flavohaemoglobin (Hmp): Reversible binding of nitric oxide and reduction to nitrous oxide. *FEBS Lett.* **445**, 389–394 (1999).
29. C. E. Mills, S. Sedelnikova, B. Søballe, M. N. Hughes, R. K. Poole, *Escherichia coli* flavohaemoglobin (Hmp) with equistoichiometric FAD and haem contents has a low affinity for dioxygen in the absence or presence of nitric oxide. *Biochem. J.* **353**, 207–213 (2001).
30. H. Arai, Regulation and function of versatile aerobic and anaerobic respiratory metabolism in *Pseudomonas aeruginosa*. *Front. Microbiol.* **2**, 103 (2011).
31. R. L. Barnard, C. A. Osborne, M. K. Firestone, Responses of soil bacterial and fungal communities to extreme desiccation and rewetting. *ISME J.* **7**, 2229–2241 (2013).
32. P. Iovieno, E. Bååth, Effect of drying and rewetting on bacterial growth rates in soil. *FEMS Microbiol. Ecol.* **65**, 400–407 (2008).

33. E. Harris *et al.*, Denitrifying pathways dominate nitrous oxide emissions from managed grassland during drought and rewetting. *Sci. Adv.* **7**, eabb7118 (2021).
34. A. H. Krichels *et al.*, Rapid nitrate reduction produces pulsed NO and N_2O emissions following wetting of dryland soils. *Biogeochemistry* **158**, 233–250 (2022).
35. P. M. Homyak *et al.*, Aridity and plant uptake interact to make dryland soils hotspots for nitric oxide (NO) emissions. *Proc. Natl. Acad. Sci. U.S.A.* **113**, E2608–E2616 (2016).
36. N. Loick *et al.*, Denitrification as a source of nitric oxide emissions from incubated soil cores from a UK grassland soil. *Soil Biol. Biochem.* **95**, 1–7 (2016).
37. M. Kolpen *et al.*, Nitric oxide production by polymorphonuclear leucocytes in infected cystic fibrosis sputum consumes oxygen. *Clin. Exp. Immunol.* **177**, 310–319 (2014).
38. J. Membrillo-Hernández, N. Ioannidis, R. K. Poole, The flavohaemoglobin (HMP) of *Escherichia coli* generates superoxide in vitro and causes oxidative stress in vivo. *FEBS Lett.* **382**, 141–144 (1996).
39. L. Y. Yeung, Combinatorial effects on clumped isotopes and their significance in biogeochemistry. *Geochim. Cosmochim. Acta* **172**, 22–38 (2016).
40. H.-L. Schmidt, R. A. Werner, N. Yoshida, R. Well, Is the isotopic composition of nitrous oxide an indicator for its origin from nitrification or denitrification? A theoretical approach from referred data and microbiological and enzyme kinetic aspects *Rapid Commun. Mass Spectrom.* **18**, 2036–2040 (2004).
41. K. L. Palmer, L. M. Aye, M. Whiteley, Nutritional cues control *Pseudomonas aeruginosa* multicellular behavior in cystic fibrosis sputum. *J. Bacteriol.* **189**, 8079–8087 (2007).
42. M. A. Spero, D. K. Newman, Chlorate specifically targets oxidant-starved, antibiotic-tolerant populations of *Pseudomonas aeruginosa* biofilms. *mBio* **9**, e01400-18 (2018).
43. K.-H. Choi, H. P. Schweizer, mini-Tn7 insertion in bacteria with single *att*Tn7 sites: Example *Pseudomonas aeruginosa*. *Nat. Protoc.* **1**, 153–161 (2006).
44. D. G. Gibson *et al.*, Enzymatic assembly of DNA molecules up to several hundred kilobases. *Nat. Methods* **6**, 343–345 (2009).
45. N. Yoshida, S. Toyoda, Constraining the atmospheric N_2O budget from intramolecular site preference in N_2O isotopomers. *Nature* **405**, 330–334 (2000).
46. F. Madeira *et al.*, Search and sequence analysis tools services from EMBL-EBI in 2022. *Nucleic Acids Res.* **50**, W276–W279 (2022).